A novel shell element for textile composite structural analysis

Wu Xu[1] and Anthony M.Waas[2]
University of Michigan, Ann Arbor, Michigan,48109

A shell element for analysis of textile composite structures is proposed in this paper. Based on the embedded element method and solid shell concept, the architecture, geometry and material properties of a Repeat Unit Cell (RUC) of textile composite are embedded in a single shell element. Flat and curved textile composite structures are used to apply and verify the present shell element. It is shown that the proposed shell element is efficienct, simple and reliable.

Nomenclature

C	=	kinematic relation between host element and embedded element, Eq.(5a)
D	=	elastic stiffness
E	=	Young's module
G	=	shear module
h	=	plate thinness
K	=	global stiffness matrix
k	=	shear factor
K_a	=	kinematic relation between plate element and solid element
$N(\zeta, \eta, \xi)$	=	shape function
P	=	effective node force given in Eqs.(6d), (12c) and (16b)
p	=	pressure acting at a element surface or edge
T	=	transfer matrix
u_i, v_i, w_i	=	transversely displacement of the ith node
α	=	a very small value used in Eqs.(13)
ε	=	strain vector
θ_{tx}, θ_{ty}	=	rotational degree of freedoms of the ith node
π	=	potential energy
v	=	Poisson's ratio

I. Introduction

Textile composites are widely used as structural materials in aerospace and automotive industrial applications. Numerical methods, especially the Finite Element Method (FEM), are increasingly used to analyze structural components made with textile composites. There are several difficulties involved in the application of traditional FEM for textile composites. In the traditional FEM[1,2], the material properties within an element are assumed to be constant, based on averaged properties. This assumption can lead to error when one solid element is used for a Repeat Unit Cell (RUC) of textile composite, where material property discontinuities are observed. In order to apply the traditional FEM, thousands of elements with constant material properties have been used to model the tows and matrix in a RUC[3]. It is costly, to analyze a textile composite structural component by modeling the entire structure as a collection of RUCs. In order to reduce the computational demand, homogenized methods have been proposed to determine the properties of a RUC. Once the homogenized material properties are obtained from the RUC, they

---

areused as constant for the whole composite structure. This method can dramatically reduce the degrees of freedom of a real composite structure. However the modeling of a RUC can be formidable depending on the extent of details to be incoportaed especially , due to the complex geometric architecture of textile RUCs. Various mesh methods and special mesh generators were designed to create finite element models for the complex geometric architecture of textile composites in Refs. [4-6]. In addition, periodic boundary conditions are usually required to obtain the elastic homogenized properties, which makes the meshing and subsequent modeling to be constrained.

This paper is concerned with the development of a shell element for analyzing thin-walled textile composite structural components. The method introduced is novel and based on the embedded element method and the general solid shell concept[7], with additional necessary features needed to reduce computational complexity while maintaining the required fidelity. The advantage of the embedded element method is that the tow and matrix of a textile composite RUC can be meshed independently, which reduces the modeling efforts and total elements significantly. Flat and curved thin structures made of textile composites are used to apply and verify the present shell element. The displacements obtained by using the present shell element are compared well with those obtained from three dimensional finite element analysis by using ABAQUS. The present method is demonstrated to be simple, efficient, accurate and reliable.

II.   The embedded element method

For simplicity, a truss element embedded in a plane element shown in Fig.1a is used to illustrate the idea of the embedded element method. The plane is modeled by one element, for example by a four node bilinear plane stress element and the truss is meshed by a truss element. The total potential energy for the system shown in Fig.1a is

$$\Pi = \Pi_p + \Pi_t \tag{1}$$

where

$$\Pi_p = \int_S \frac{1}{2}\varepsilon_p^T D_p \varepsilon_p \cdot \mathrm{d}s - \int_L u_p^T \cdot p \cdot \mathrm{d}l \tag{2a}$$

$$\Pi_t = \int_L \frac{1}{2}\varepsilon_t^T D_t \varepsilon_t \cdot A\mathrm{d}l \tag{2b}$$

Following the finite element method, the displacement fields in the plane and truss element are interpolated as follows.

$$u^p = \sum_{i=1}^{4} N_i(\xi,\eta) \cdot u_i^p \tag{3a}$$

$$u^t = \sum_{i=1}^{2} N_j(\xi) \cdot u_j^t \tag{3b}$$

The subscript and superscript p and t in Eqs.(2-3) are used to represent the plane element and truss element, respectively. u_i is the displacement at the ith nodes. $N(\xi)$ and $N(\xi,\eta)$ are the shape function for the two node truss element and four noded plane element, respectively.

For the considered example, the displacements at node $1(x_1, y_1)$ and 2 (x_2, y_2) of the truss element should equal those at the same location of the plane element, which leads to

$$\left[u_1^t, v_1^t, u_2^t, v_2^t \right]^T = \left[C \right] \cdot \left[u_1^p, v_1^p, u_2^p, v_2^p, u_3^p, v_3^p, u_4^p, v_4^p \right]^T \tag{4}$$

where

$$C = \begin{bmatrix} a_1 & 0 & a_2 & 0 & a_3 & 0 & a_4 & 0 \\ 0 & a_1 & 0 & a_2 & 0 & a_3 & 0 & a_4 \\ b_1 & 0 & b_2 & 0 & b_3 & 0 & b_4 & 0 \\ 0 & b_1 & 0 & b_2 & 0 & b_3 & 0 & b_4 \end{bmatrix} \tag{5a}$$

$$a_i = N_i(x_1, y_1), \ b_i = N_i(x_2, y_2), \ i=1,2,3,4 \tag{5b}$$

Substituting Eqs.(2-5) into Eq.(1) and using the principle of minmum potential engery leads to

2
American Institute of Aeronautics and Astronautics

$$[K]\{u\} = \{P\} \tag{6a}$$

where,

$$K = K^p + K^{em} \tag{6b}$$

$$K^{em} = C^T \cdot K^t \cdot C \tag{6c}$$

$$P = \int_L N(\xi) \cdot p(\xi) \cdot \mathrm{d}l \tag{6d}$$

$$\{u\} = \left[u_1^p, v_1^p, u_2^p, v_2^p, u_3^p, v_3^p, u_4^p, v_4^p \right]^T \tag{6e}$$

The kinematic relation matrix C is given in Eq.(5). The stiffness matrix of the plane (K_p) and truss (K_t) elements and load vector P are the same as those obtained by using the regular finite element method.

It is noteworthy that 1) The total Degrees of Freedom (DoF) of the system is equal to that of the plane element and 2) the contribution of the embedded truss is included in the global stiffness matrix through the kinematic relation matrix C given in Eq.(5). As a result, the advantage of this method is its reduction of global DoF. This advantage is very attractive for global-local or multi-scale analysis. Another advantage of this method is that the embedded elements (the truss element) do not require common nodes with the host element (plane element in this case). This means that the embedded element and host element can be separately meshed. This advantage is very appealing for complex textile architectures such as angle interlock weaves.
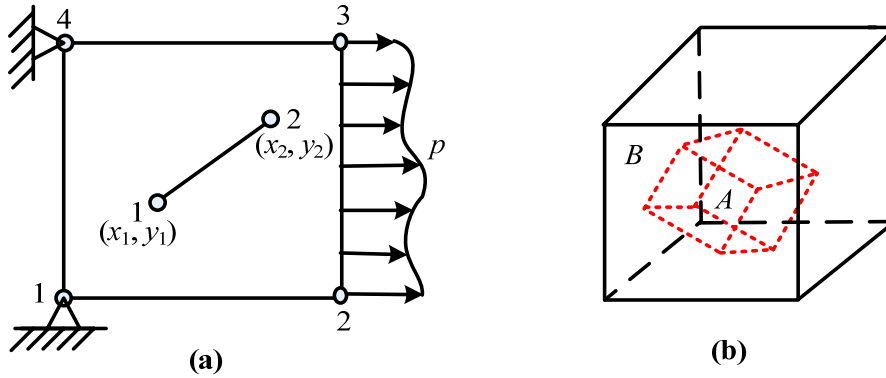
Figure 1. Embedded elements examples: (a) A truss element embedded in a plane element; and (b) A solid element embedded in another solid.

The embedded element method can be easily extended to analyze a three dimensional case. A solid element A embedded in a large solid element B is shown in Fig.1b. However, the volume effect of the solid A should be well considered. In practice, the material properties of the host element B is unchanged, while equivalent elastic stiffness D given in Eq.(7) for the embedded solid A are used for applying this method.

$$\{\sigma\} = [D]\{\varepsilon\} = ([D_A] - [D_B]) \cdot \{\varepsilon\} \tag{7}$$

where, D_A and D_B represent the elastic stiffness of the solids A and B, respectively.

The single-field macro-element presented in Ref.[8] and the domain superposition technique given in Ref.[9] and the present embedded element method share many similarities. However, to the knowledge of the authors, there is no literature using the embedded element method to design shell elements for structural analysis of textile composite structures.

III.   Derivation of plate element from solid element

Derivation of shell element from solid element was originally proposed by Ahmad et al.[7]. Subsequently, various "solid" shell elements were proposed. This idea is implemented in this paper. For simplicity, an eight noded solid element shown in Fig.2a is used to illustrate the derivation of the shell element. The potential energy of the solid element shown in Fig.2a is

American Institute of Aeronautics and Astronautics

$$\Pi = \frac{1}{2}\int_{\Omega}\varepsilon^T D\varepsilon \cdot dV - \int_S p \cdot u \cdot ds \qquad (8)$$

Using shape functions, the displacement field in the solid element is

$$u = \sum_{i=1}^{8} N_i\left(\xi,\eta,\zeta\right)\cdot u_i \qquad (9a)$$

$$v = \sum_{i=1}^{8} N_i\left(\xi,\eta,\zeta\right)\cdot v_i \qquad (9b)$$

$$w = \sum_{i=1}^{8} N_i\left(\xi,\eta,\zeta\right)\cdot w_i \qquad (9c)$$

where $N\left(\xi,\eta,\zeta\right)$ are the shape function for an eight node solid element, and u_i, v_i and w_i are the displacement components of the ith node.

$$\begin{cases} u_1 = u_{1m} - h/2 \cdot \theta_{1y} \\ v_1 = v_{1m} - h/2 \cdot \theta_{1x} \\ w_1 = w_{1m} \\ \cdots \cdots \end{cases}$$

(a) Solid element
(b) Plate element
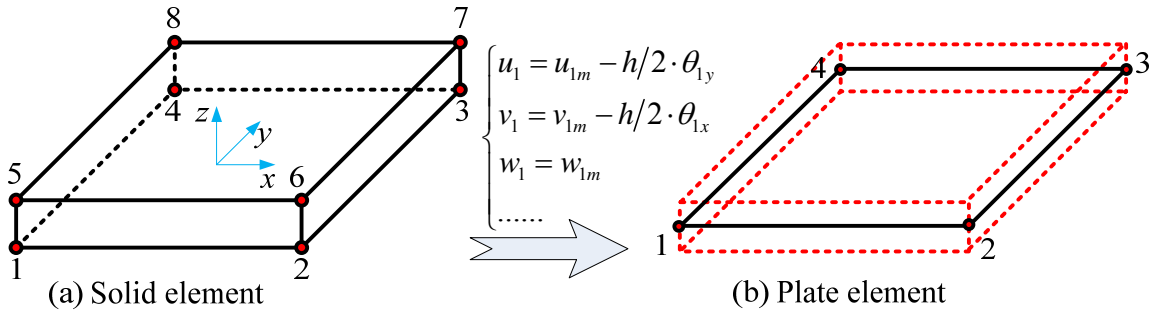
Figure 2. Derivation of plate element from solid element: (a) an eight node solid element; and (b) a four node plate element.

Plate element can be used to model the same problem shown in Fig.2a as well. The differences between the solid element and the Mindlin plate element are the kinematic assumption and stress assumption. The Mindlin plate assumes that plane sections initially normal to the neutral surface remain plane after deformation and stress normal to the neutral surface is zero. These two types of element are always designed separately. In this section, the plate element will be derived from the solid element.

According to the kinematic assumption of the plate, the displacement relationship between the solid and plate element shown in Fig.2 is given as follows.

$$\left\{u_s^e\right\} = K_a \cdot \left\{u_m^e\right\} = \begin{bmatrix} K_1 & & & & & & & \\ & K_1 & & & & & & \\ & & K_1 & & & & & \\ & & & K_1 & & & & \\ K_2 & & & & & & & \\ & K_2 & & & & & & \\ & & K_2 & & & & & \\ & & & K_2 & & & & \end{bmatrix} \cdot \left\{u_m^e\right\} \qquad (10a)$$

$$K_1 = \begin{bmatrix} 1 & 0 & 0 & 0 & -h/2 \\ 0 & 1 & 0 & h/2 & 0 \\ 0 & 0 & 1 & 0 & 0 \end{bmatrix} \quad K_2 = \begin{bmatrix} 1 & 0 & 0 & 0 & h/2 \\ 0 & 1 & 0 & -h/2 & 0 \\ 0 & 0 & 1 & 0 & 0 \end{bmatrix} \qquad (10b)$$

4
American Institute of Aeronautics and Astronautics

$$\left\{ u_s^e \right\} = \left[u_1, v_1, w_1, u_2, v_2, w_2, ..., u_8, v_8, w_8 \right]^T \tag{10c}$$

$$\left\{ u_m^e \right\} = \left[u_{1m}, v_{1m}, w_{1m}, \theta_{1x}, \theta_{1y}, ..., u_{4m}, v_{4m}, w_{4m}, \theta_{4x}, \theta_{4y} \right]^T \tag{10d}$$

where u_{im}, v_{im} and w_{im} are the transversely displacements, and θ_{ix} and θ_{iy} are the rotational degree of freedoms of the ith node of the plate element. The plate thickness is denoted by h. Substituting Eqs.(10) and the shape function $N_i(\xi, \eta, \zeta)$ for the eight noded solid element into Eqs.(9), leads to the following relations

$$u = \sum_{i=1}^{4} N_i\left(\xi, \eta\right) \cdot u_{im} + \frac{h\zeta}{2} \sum_{i=1}^{4} N_i\left(\xi, \eta\right) \cdot \theta_{iy} \tag{11a}$$

$$v = \sum_{i=1}^{4} N_i\left(\xi, \eta\right) \cdot v_{im} - \frac{h\zeta}{2} \sum_{i=1}^{4} N_i\left(\xi, \eta\right) \cdot \theta_{ix} \tag{11b}$$

$$w = \sum_{i=1}^{4} N_i\left(\xi, \eta\right) \cdot w_{im} \tag{11c}$$

where $N(\xi, \eta)$ is the shape function of four noded plane element. It is found that the displacement field given in Eq.(11) is exactly the same as that derived directly from the Mindlin plate. Substituting Eqs.(9) and Eqs.(10) into Eq.(8) and using degenerated constitutive material law which was based on zero stress component in the normal direction, the resulting potential energy is the same as that of the classical Mindlin plate element. Using the minimum potential energy principle, the following relationship is obtained.

$$\left[K_m \right] \cdot \left\{ u_m^e \right\} = \left\{ P \right\} \tag{12a}$$

where

$$K_m = K_a^T \cdot K_s \cdot K_a \tag{12b}$$

$$P = K_a^T \cdot P_s \tag{12c}$$

K_m is the stiffness matrix for the plate element, K_s is the stiffness obtained by using the regular finite element method for solid element. P and P_s are the load vector at the element node of the plate and solid element. It should be noted that in calculating K_s, all the procedure are the same as the regular finite element method excepting the elastic stiffness. Degenerated elastic stiffness should be used for K_s. For isotropic material, the degenerated elastic stiffness is

$$D = \begin{bmatrix} \dfrac{E}{1-v^2} & \dfrac{vE}{1-v^2} & 0 & & & \\ \dfrac{vE}{1-v^2} & \dfrac{E}{1-v^2} & 0 & & & \\ 0 & 0 & \alpha & & & \\ & & & G & & \\ & & & & kG & \\ & & & & & kG \end{bmatrix} \tag{13}$$

where α is a small positive value to extend the matrix size, and k is a shear factor, which for a rectangular cross-section equals 5/6.

For anisotropic material, the elastic stiffness properties are firstly transfer to the thickness direction by using Eq.(14a). Based on zero stress component in the thickness direction, the material properties are further degenerated by using Eq.(14b). The elastic stiffness D^s given by Eq.(14b) is used to obtain K_s for the solid element.

$$D = \left[T \right]^T \cdot \left[D_m \right] \cdot \left[T \right] \tag{14a}$$

5
American Institute of Aeronautics and Astronautics

$$
\begin{cases}
D_{ij}^s = D_{ij} - \dfrac{D_{i3} \cdot D_{3j}}{D_{33}} ; i, j \neq 3 \\[2ex]
D_{ij}^s = \alpha ; i \text{ or } j \neq 3
\end{cases}
\qquad (14b)
$$

In Eq.(14a), D_m is the elastic stiffness given in the material coordinate. And the matrix T can be obtained by using the equation given in Ref.[10].

It is found that the displacement field of the solid element obtained by using the present method is exactly the same as that of a four noded Mindlin plate element. The problem in the design of Mindlin plate element is shear locking. Various methods were proposed to avoid shear locking. Among these methods, the selective reduced integration method was widely used to remedy shear locking[2]. Since this method is simple and efficient, it is applied here to determine the stiffness for K_s.

It is observed that the derivation of the plate element from the solid element is more complicated than that directly based on the Mindlin plate theory. However, the strength of this method is its ability to analyze complex textile composite microstructures, which will be demonstrated in the following.

IV.   Derivation of shell element for textile composite structure

In this section, the methods described in the previous sections are used to design plate and shell elements for textile composite structures.

A. Plate element for textile composite

Figure 3 shows a RUC of waving textile composite. The matrix is not shown in this figure. The undulating tow follows a sinusoidal path given by, $1.0\sin(\pi/8)$ mm. The major and minor axes of the elliptical cross-section of the tow are 6.0 mm and 1.5 mm, respectively. The width and thickness of the square RUC are 16 mm and 3.8 mm.
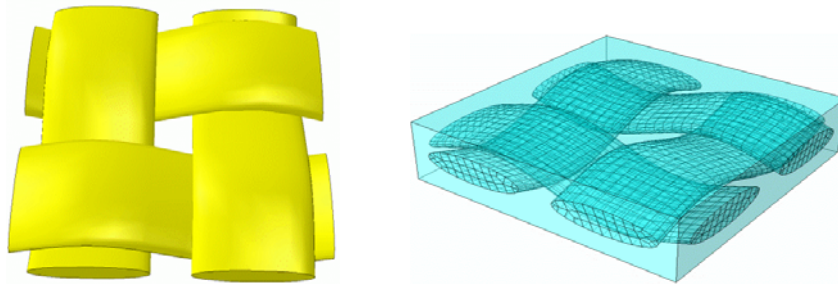
Figure 3. A Representative Unit Cell of waving textile composite: (a) geometrical dimension;

and (b) mesh of the RUC.

Combination of the methods described in sections 2 and 3, results in a plate element for the RUC. An eight noded plate element is used to demonstrate the process shown in Fig.4. Detailed interpretation of the procedure is given as follows;

1)   Element definition; Like doing finite element analysis by using commercial software, the finite element node location, element type and element connectivity are defined based on the geometrical information from a given problem. The difference in the present study are that: 1) the matrix is assumed to fully occupy the RUC (16mm×16mm×3.8mm) volume; and 2) the tow and matrix are separately meshed, which means that these is no requirement for common nodes between the tow and matrix. Figure 3b shows the mesh of the tow and matrix, where the matrix is model by a twenty noded solid element, while hundreds of twenty noded solid elements are used for the tows. In the practical application of the present method (section 5), sixteen elements (4×4×1) are used for the matrix.

2)   Material properties; The matrix is always assumed to be an isotropic solid, while the tow made up of fiber and matrix are frequently modeled as transversely isotropic solid. As a result, a coordinate system for the tow is required to define the material properties variation as the tow undulates. In order to apply the present method, equivalent material properties are required to consider the volume effect (the matrix is assumed to be full of the RUC) by using Eq.(7). Then, the elastic stiffness of matrix and tow are further degenerated by using Eq.(13)

and (14), respectively. It is noteworthy that for the present tows, D_m in Eq.(14) is the equivalent property given by Eq.(7).

3) Stiffness matrix determination for the tow and matrix; Using the regular finite element method, the element information in step (1) and material properties obtained in step (2), the stiffness matrix for each element of the tow and matrix can be obtained. In order to remedy shear locking, selective reduced integration method is used to obtain the element stiffness for the matrix. Due to the coupling between shear and normal strain, it is difficult to distinguish the shear strain energy between bending and tension energy for the tow. As a result, reduced integration is used to obtain the element stiffness for tows. Usually, the rank deficiency introduced by the reduced integration method can be remedied by using many finite elements. In the examples presented in section 5, rank deficiency is not observed.

4) Determination of C matrix; The shape function for a sixteen noded solid element can be obtained by using the method given in Ref.[2]. Once the shape function is obtained, the C matrix and the embedded stiffness matrix K_{em} can be determined. The stiffness of the sixteen noded solid element Ks, shown in Fig.4b, is obtained by summing all of K_{em}.

5) Determination of the stiffness of plate element; Using Eq.(10a) to obtain the kinematical relationship matrix K_a and K_s obtained in step (4), the stiffness of the corresponding eight noded plate element is finally obtained by using Eq.(12b).
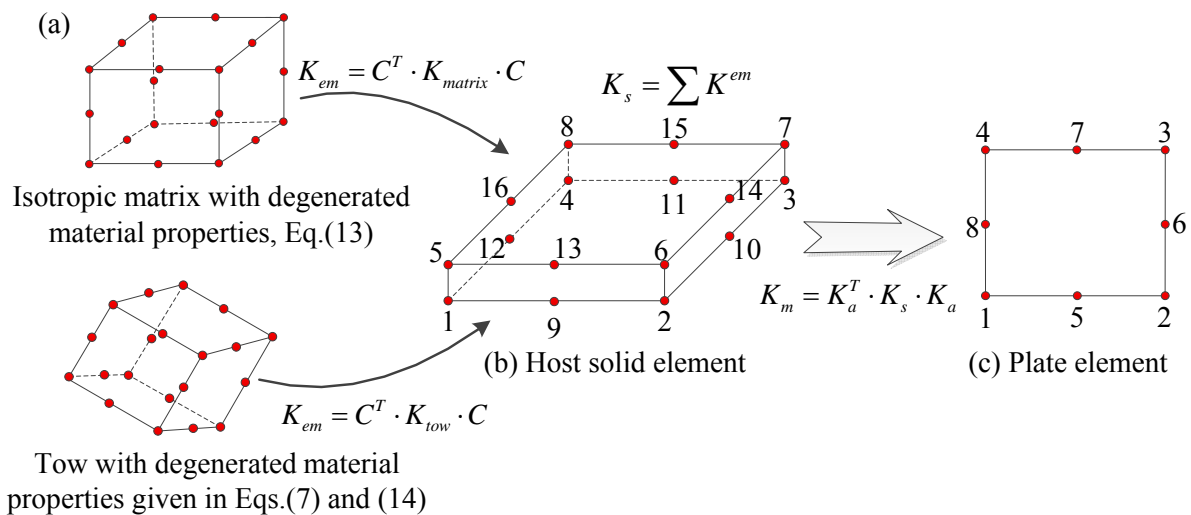
Figure 4. Procedures for the design of plate element for textile composites.

B. Shell elements for textile composite

Shell structures are frequently analyzed as an assembly of flat plate elements[11]. Besides the five degrees of freedom at each node, a drilling rotation θ_z is included to extend the plate element to analyze curved structures. This means the size of the element stiffness matrix is extended from $5n \times 5n$ to $6n \times 6n$, where n is the number of element nodes. The zero stiffness matrix corresponding to θ_z results in the singularity in the global stiffness matrix. To deal with this difficulty, the simple approach given in Ref.[11] is adopted here. An arbitrary small stiffness coefficient K_{θ_z} at the additional degree of freedom θ_z is added in the extended element stiffness matrix.

The element stiffness and load vector for the plate element are determined in terms of a local coordinate system that has x and y axes along the mid-plane and z axis normal to the plane. In order to assemble these matrix and vectors into the global stiffness matrix and load vector, the nodal degree of freedom in terms of the local coordinates must be transformed into those in terms of the global coordinate system. At each node, the relation between the local and global degree of freedom is

$$\left\{ u^{global} \right\} = \left[T_l \right] \left\{ u^{local} \right\} \tag{15}$$

T_l is the transform matrix, which consists of the direction cosines between the global axis and the corresponding local axis. The element stiffness matrix K and load vector P in the global coordinates are given as follows.

7

American Institute of Aeronautics and Astronautics

$$K = T_g^{\ T} \cdot K^e \cdot T_g \tag{16a}$$

$$\{P\} = \left[T_g\right]^T \cdot \left\{P^e\right\} \tag{16b}$$

where

$$T_g = \begin{bmatrix} T_l & & & \\ & T_l & & \\ & & \ddots & \\ & & & T_l \end{bmatrix} \tag{16c}$$

The size of T_g is dependent on the node number of element. There are eight T_l for eight noded shell shown in Fig.4c.

V. Applications and verifications

Three test examples shown in Fig.5 are used to apply and verify the present method. The first one shown in Fig.5a is a square plate made of isotropic material. It is used to apply and verify the method introduced in section 3, which is the derivation of plate element from solid element. The next two examples are flat and curved sheets made of textile composite. They are used to demonstrate and verify the present plate and shell element for textile composite structures. Some of the matrix shown in Fig.5b and c are removed to show the architecture of the tows.
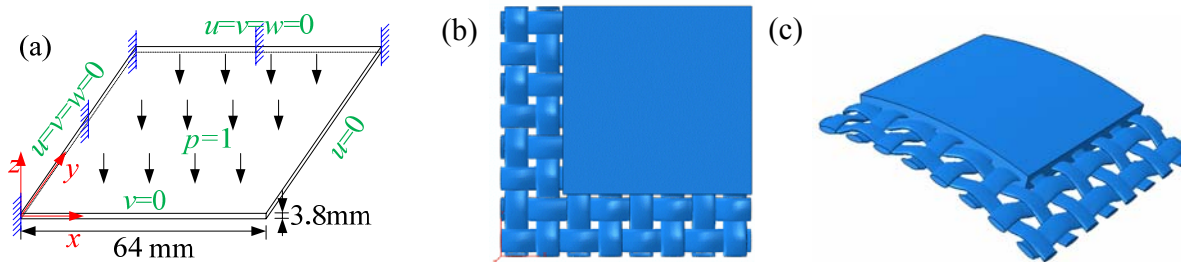
Figure 5. Test examples: (a) An isotropic plate; (b) a flat textile composite sheet; and (c) a curved textile composite sheet

A. Isotropic square plate

A square aluminum plate subjected to uniform pressure p (p=1) and clamped boundary conditions is analyzed by using the present plate element. The material properties are elastic modulus, E=70Gpa, Poisson' ratio v=0.3. The width and thickness of the plate are 128mm and 3.8mm, respectively. Due to the symmetry, one quarter of this plate shown in Fig.5a is modeled and analyzed. In order to obtain the reference solution to this problem, higher order solid elements and shell elements given in ABAQUS® are used. The out of plane displacement at the plate center (x=64mm, y=0mm, z=0mm shown in Fig.5a) is found to converge to -0.98mm. The analytical result based on Kirchhoff–Love assumption is -0.96mm[12]. Since the transverse displacement caused by shear strain is considered by ABAQUS®, the displacement is slightly larger than that of the analytical result (-0.96mm).

Having obtained the reference solution to the problem shown in Fig.5a, the method described in section 2 is used to design a plate element to solve this problem. Sixty elements are uniformly meshed for one quarter of the plate. Firstly, an eight noded solid element is used to derive a four noded shell element, degenerated material properties given in Eq.(13) are used. Reduced integration method for the shear strain energy is used to obtain the stiffness matrix of the solid element (K_s) to avoid shear locking. The stiffness of the plate element is then determined by using the kinematical relationship given in Eq.(10a) and (12b). Once the stiffness of the plate element is determined, the deformation of the problem shown in Fig.5a can be solved by following the regular finite element method. The out of plane displacement obtained by the present plate element S4S is given in Table 1. It is observed that the present result agrees very well with that obtained from ABAQUS. If the reduced integration method is used for all the strain energy, the result is also presented in Table 1, see the S4R column. The result from S4R is more flexible than that from the S4S element.

American Institute of Aeronautics and Astronautics

Table 1 Displacement results for an isotropic plate, material properties are degenerated

Element types	S4R	S4S	S8S	S8R	ABAQUS
Results	-1.17	-0.98	-0.98	-0.98	-0.98

A sixteen noded solid element is also used to derive an eight noded plate element. Reduced integration method and degenerated material properties are used. Two types of eight noded plate elements are used. The difference between these two elements is the integration method for calculating the stiffness of solid. Selective reduced integration method is used only for the shear strain energy for S8S; while for S8R, reduced integration method is used for all the strain energy. The corresponding results are given in Table 1 as well. It is observed that the results from the two types of elements compare very well with the ABAQUS results.

B. 5.2 Flat textile composite plate

Figure 5b shows a textile composite plate. The tow and matrix are respectively assumed to be transversely isotropic and isotropic solids. The dimension, boundary and loading conditions of the textile plate are the same as that of the isotropic aluminum plate shown in Fig.5a. The textile plate shown in Fig.5b is made up of sixteen RUCs. The geometrical architecture of a RUC is the same as that shown in Fig.3a. The mechanical properties of the tow and matrix are given in Table 2. The elastic modulus of the matrix is assumed to be a spurious large value to verify whether the volume effect is adequately captured using (Eq. 7).

Table 2 Material properties for the tow and matrix

Transversely isotropic tow					Isotropic matrix	
E_1	E_2	G_{12}	G_{23}	v_{12}	E	v
180Gpa	60Gpa	64Gpa	23Gpa	0.4	40Gpa	0.3

The stiffness and load vector of an eight noded plate element S8 for the RUC shown in Fig.3a is obtained by following the method introduced in Section 4.1. Subsequently, sixteen (4×4) plate elements are used to analyze the textile composite plate. The out of plane displacement at (x=64mm, y=0mm, z=0mm) is -1.16mm given in Table 3. In order to verify the present method, a full three dimensional finite element analysis is carried out by using ABAQUS[®]. Since the architecture of the textile plate is very complex, the C3D10 element is used and the out of plane displacement at the plate center has a converged value of -1.28mm.

Table 3 Results from different types of elements, 4×4 shell elements

Element type	S8R	S9R	S12R	S16R	S25R	Full 3D (C3D10)
displacement	-1.16	-1.17	-1.18	-1.21	-1.25	-1.28

There are two ways to improve the accuracy. These are, (a) using high order finite elements, and (b) making the mesh finer. Since the displacement field in a RUC is very complex, higher order plate finite elements are required to improve the accuracy. The element type and mesh size of the tow and matrix are the same as that of S8 (as shown in Fig.3b). Higher order plate elements for textile plates can be achieved by increasing the node number of the host solid element shown in Fig.5b. Four types of higher order solid elements with eighteen, twenty-four, thirty-two, and fifty nodes are used to design a higher order plate element. By following the method described in section 4.1, the corresponding plate elements S9, S12, S16 and S25 are designed and applied to solve the textile plate transverse loading problem. The out of displacement obtained by using the four types of elements are shown in Fig.6. The solid line shown in this figure is the result obtained from full three dimensional analysis. For comparison, the out of displacements at (x=64mm, y=0mm, z=0mm) are given in Table 3. It is observed that the results obtained from plate elements converge to the reference values as the element order increases.
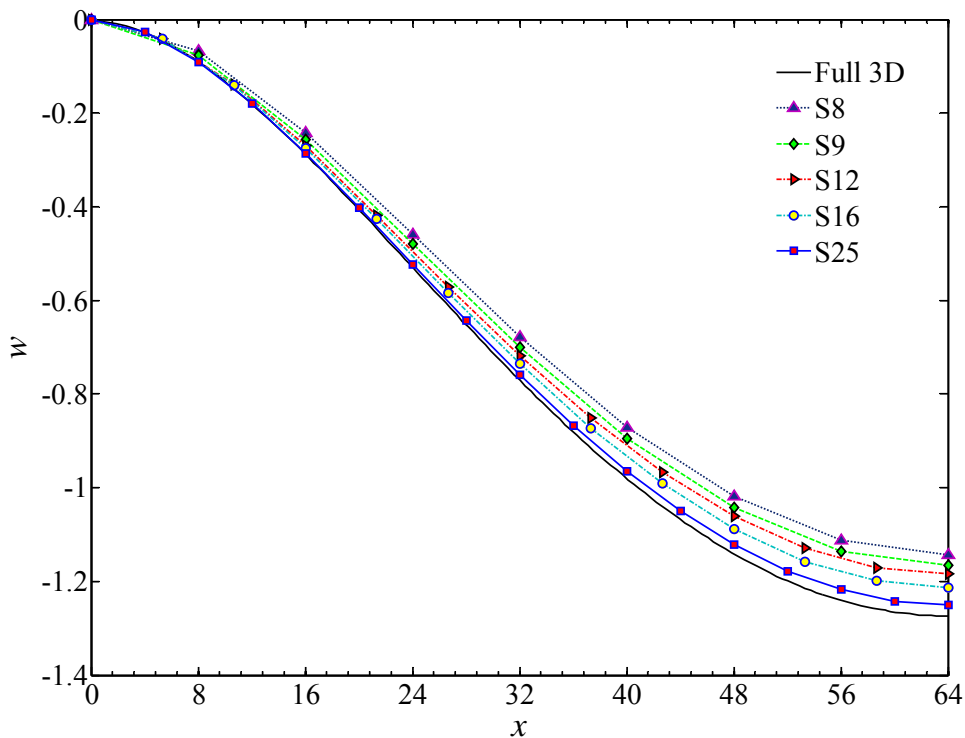
Figure 6. Comparison of the deformation in the thickness direction along *x*, *y*=0 between plate element and three dimensional analysis by using C3D10, the plate is uniform meshed by 4×4 elements.

C. Curved textile composite structure

A curved structure made of a woven textile composite is shown in Figs.7 and 5c. It consists of sixteen RUCs. A three dimensional architecture of the curved shell structure is shown in Fig.5c. The major and minor axes of the elliptical cross-section of the tow are 2.4 mm and 0.6 mm, respectively. The axes of the tow and matrix follow the paths shown in Fig.7c. The boundary conditions are: Fixed boundary displacement is applied along the edge *AB* shown in Fig.7b; and the top surface of the curved shell is subjected to uniform pressure *p*=0.1Mpa, Fig.7a. The tow is made up of carbon fiber and epoxy matrix, the corresponding properties and volume fraction v_f are given in Table 4[13]. Using micro-mechanics method and the Concentric Cylinder Model described in Refs.[13-16], the properties of the tow is calculated by using the equations given in Ref.[16] and given in Table 5.

Table 4 The mechanical properties of carbon fiber and epoxy material

Transversely isotropic carbon fiber						Isotropic epoxy matrix		
E_1(Gpa)	E_2(Gpa)	G_{12}(Gpa)	G_{23}(Gpa)	v_{12}	v_f	E(Gpa)	v	v_m
231.0	15.0	24.0	5.01	0.14	0.6	3.0	0.36	0.4

Table 5 Calculated mechanical properties of the tow by using CCM

E_1(Gpa)	E_2(Gpa)	G_{12}(Gpa)	G_{23}(Gpa)	v_{12}
139.84	6.40	3.77	2.36	0.22

The problem in Fig.7a is modeled by 4×4 shell elements shown in Fig.7b. A shell element with 25 nodes is designed following the method introduced in section 4. Once the stiffness and load vector of the shell element are obtained, the displacement can be obtained by following the procedure of the regular finite element method. The square symbol shown in Figure 8 indicates the variation of the displacement in the *z* direction with respect to the angle θ. In order to verify the present results, the corresponding results from a full three dimensional analysis with more than 220,000, C3D10 elements are also given in Fig.8. The difference between these two results is within 6%.

American Institute of Aeronautics and Astronautics

However, the present shell element is much more efficient than the traditional full three dimensional finite element analysis.

(a) Geometry and load

(b) Mesh and BC

(c) Arckitecture of tow

$$\begin{cases} x = R\sin\theta \\ z = R\cos\theta; \theta \in [0, \pi/6] \end{cases} \text{matrix}$$

$$\text{tow} \begin{cases} x_t = [R + r\sin(48\theta)] \cdot \sin\theta \\ z_t = [R + r\sin(48\theta)] \cdot \cos\theta \\ r = 1.0; \theta \in [0, \pi/6] \end{cases}$$

$l_{AB} = 64.0$

$R = 8.0/\sin(\pi/48)$

$\theta = \pi/6$
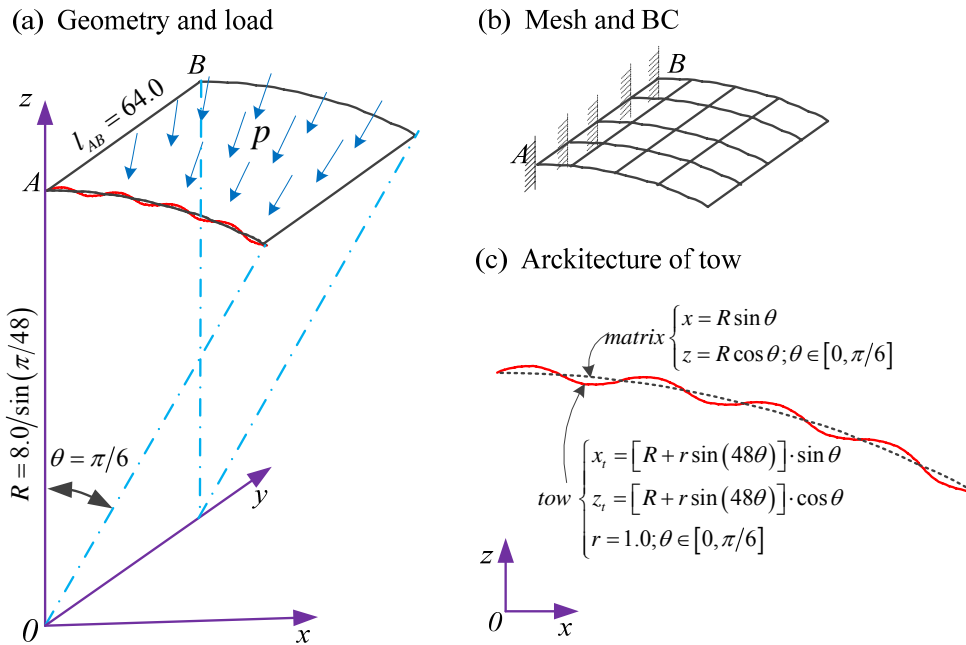
Figure 7. A curved shell made of waving textile composite subjected to uniform pressure and fixed displacement at one edge.
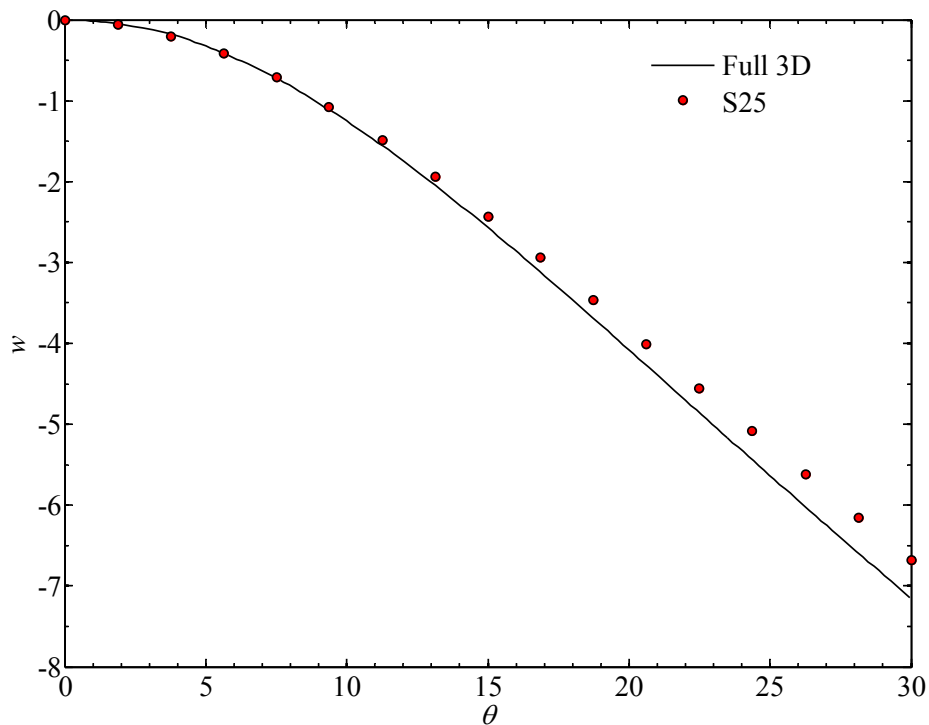
Figure 8. Variation of the displacement component in z direction with angle θ.

11

American Institute of Aeronautics and Astronautics

It is observed that the present example is a multi-scale analysis of textile composite structure. The inputs are the material properties and volume fractions of the fiber and matrix (micro-scale), the architecture of the tow (meso-scale), geometrical and loading conditions of the textile composite structure (macro-scale). The output is the deformation response of the structure. The strength of the present method is that once the inputs are available, the deformation of a real textile composite structure can be quickly obtained without sacrificing accuracy.

VI. Conclusions

In this paper, new shell elements are derived for analysis of textile composite structures. The architecture, geometries and material properties of a RUC are embedded in a single shell element. The present plate and shell elements are validated by flat and curved structures made of textile composites. Compared to the traditional finite element method for textile composites, the present shell element has the following characteristics;

1) Modeling efficiency. The tow and matrix in a RUC are meshed independently. It results in fewer elements in a RUC and free of needs associated with special mesh generation

2) Computational efficiency. Once a shell element is designed, it can significantly reduce the total number of degrees of freedom of a composite structure, analyzed using a standard FEM

3) Simple. The design of the shell element is quite simple. It is mainly based on the shape function and kinematic relationship matrix. No new knowledge of the finite element method is required.

4) Reliable. Like the traditional FEM, the displacement results obtained from the present shell element converge to the exact value with an increase in element order.

References

[1]ABAQUS. ABAQUS 6.11 Documentation. Dessault systems

[2]Hughes, T. J. R., Finite Element Method: Linear Static and Dynamic Finite Element Analysis. Dover Publications, Inc.2000

[3]Song, S. J, Waas, A.M., Shahwan, K.W., Faruque, O., and Xiao, X.R., "Compression response of 2D braided textile composites: single cell and multiple cell micromechanics based strength predictions," Journal of composite materials, Vol.42, No. 23, 2008, pp. , 2461, 2482.

[4]Verpoest, I., and Lomov, S. V., "Virtual textile composites software WiseTex: Integration with micro-mechanical, permeability and structural analysis," Composites Science and Technology, Vol.65, 2005, pp., 2563, 2574.

[5]Sun, W., Lin, F., and Hu, X., "Computer-aided design and modeling of composite unit cells," Composites science and technology, Vol. 61, 2001, pp. 289, 299.

[6]Lin, H., Zeng, X.S., Sherburn, M., Long, A.C., and Clifford, M.J., "Automated geometric modeling of textile structures," Textile research Journal,Vol. 82,No.16, 2011, pp., 1689,1702.

[7]Ahmad, S., Bruce M. and Zienkiewicz, O.C., "Analysis of thick and thin shell structures by curved finite elements," International Journal for numerical method in engineering,Vol. 2, 1970, pp., 419,451.

[8]Woo, K. and Whitcomb, J. D., "A post-processor approach for analysis of woven textile composites," Composites science and technology , Vol.60, 2000, pp., 693,704.

[9]Jiang,W.G., "Implementation of domain superposition technique for the nonlinear analysis of composite materials," Journal of composite materials, 2012, pp., 1,7.

[10]Ting, T.C.T. , Anisotropic elasticity theory and applications. New York, Oxford university press, 1996.

[11]Zienkiewicz, O.C., and Taylor, R.L., The Finite Element Method: Vol.2 Solid mechanics, 5th ed., Butterworth Heinemann, Oxford, 2000.

[12]Timoshenko,S., and Woinowsky-Krieger, S., Theory of plates and shells. McGraw-Hill,1959.

[13]Quek,S.C., Waas,A.M, Shahwan, K.M, and Agaram,V., "Analysis of 2D triaxial flat braided textile composites," International journal of mechanical sciences,Vol. 45, 2003, pp.,1077,1096.

[14]Hashin, Z., and Walter Rosen, B., "The elastic moduli of fiber-reinforced materials," Journal of Applied Materials, 1964, pp., 223,232.

[15]Christensen, R.M., Mechanics of composite materials, John Wiley & Sons. New York, New York.1979.

[16]Zhang, D., and Waas, A. M., "A micromechanics based multiscale model for nonlinear composite", Acta Mechanica (to be published).